Anticrossing and coupling of light-hole and heavy-hole states in (001) GaAs/$Al_xGa_{1-x}As$ heterostructures

Rita Magri
Istituto Nazionale per la Fisica della Materia e Dipartimento di Fisica, Università di Modena e Reggio Emilia, Modena, Italy

Alex Zunger
National Renewable Energy Laboratory, Golden, Colorado 80401
Received 15 May 2000)

Heterostructures sharing a common atom such as AlAs/GaAs/AlAs have a D_{2d} point-group symmetry which allows the bulk-forbidden coupling between odd-parity light-hole states e.g., lh1) and even-parity heavy-hole states e.g., hh2). Continuum models, such as the commonly implemented ''standard model'') $\mathbf{k}\cdot\mathbf{p}$ theory miss the correct D_{2d} symmetry and thus produce zero coupling at the zone center. We have used the atomistic empirical pseudopotential theory to study the lh1-hh2 coupling in 001) superlattices and quantum wells of GaAs/$Al_xGa_{1-x}As$. By varying the Al concentration x of the barrier we scan a range of valence-band barrier heights $E_v(x)$. We find the following: i) The lh1 and hh2 states anticross at rather large quantum wells width or superlattice periods $60<n_c<70$ monolayers. ii) The coupling matrix elements $V^{\mathbf{k}_\parallel=0}_{lh1,hh2}$ are small 0.02–0.07 meV) and reach a maximum value at a valence-band barrier height E_v 100 meV, which corresponds to an Al composition $x_{Al}=0.2$ in the barrier. iii) The coupling matrix elements obtained from our atomistic theory are at least an order of magnitude smaller than those calculated by the phenomenological model of Ivchenko *et al.* Phys. Rev. B **54**, 5852 1996)]. iv) The dependence of $V_{lh1,hh2}$ on the barrier height $E_v(x)$ is more complicated than that suggested by the recent model of Cortez *et al.*, J. Vac. Sci. Technol. B **18**, 2232 2000)], in which $V_{lh1,hh2}$ is proportional to the product of $E_v(x)$ times the amplitudes of the lh1 and hh2 envelopes at the interfaces. Thus, atomistic information is needed to establish the actual scaling.

I. INTRODUCTION

A. The three classes of light-hole–heavy-hole coupling in semiconductor heterostructures

Quantum states that belong to the same symmetry representation mix and anticross in the presence of a perturbation. The anticrossing effect on electronic energy levels of solids is often very significant, and includes the occurrence of ''band-gap bowing'' in random alloys,[1] band-gap narrowing in ordered vs random alloys,[2] saturation of impurity levels with pressure,[3] and ''*p-d* repulsion'' in II-VI Ref. 4) or I-III-VI_2 Ref. 5) compounds affecting band offsets and spin-orbit splitting. Here we focus on the consequences of level anticrossing in 001) semiconductor superlattices and quantum wells made of zinc-blende constituents. In the zinc-blende structure the valence-band maximum VBM) is a four-degenerate $_{8v}$ state including~hh!components. The optical transitions lh1 to the first electron level e are allowed in the bulk and have isotropic polarization. When one forms a 001)-oriented quantum well from zinc-blende components, there are three different effects on the electronic states: i) The zinc-blende bands between (000) and X(001) fold into $\mathbf{k}$

$_\parallel=0$ of the quantum well thus adding new states, ii) the reduced superlattice symmetry from T_d can split $_{8v}$, and iii) the strain arising from size mismatch can also split $_{8v}$. This last effect is absent in lattice-matched components such as GaAs and AlAs. In GaAs/AlAs heterostructures effects i) and ii) give rise to a series of hole levels hh1<lh1<hh2 . . . and electron states $e1<e2<\ldots$ at $\mathbf{k}_\parallel=0$.

Coupling exists between states of the same symmetry. This is decided as follows. A *single* zinc-blende 001) interface has C_{2v} symmetry.[6] If one forms a structurally perfect

ropy 0. The nature of the level mixing depends on symmetry. There are three cases: i) A single zinc-blende interface; the symmetry is C_{2v}. ii) Two different interfaces in systems that do not share a common atom; the symmetry is C_{2v}. iii) Two interfaces in systems that share a common atom; the symmetry is D_{2d}. Two equal interfaces in no-common atom systems in 001) superlattices with a noninteger period also have D_{2d} symmetry. We next describe briefly these cases summarized in Table I. In this paper we concentrate mainly on case iii).

i) *A single zinc-blende interface:* C_{2v}. A single interface

hand, the $\mathbf{k}\cdot\mathbf{p}$ theory is capable of describing couplings at $\mathbf{k}_{\|}$ 0 and thus has produced results similar to those of atomistic theories for the hibridization gaps at $\mathbf{k}_{\|}$ 0 in nominally semimetallic $(\mathrm{InAs})_n/(\mathrm{GaSb})_n$ superlattices with $n > 28$.[16]

iii) *Two interfaces of a common-atom heterostructure:* D_{2d}. The states that have the same symmetry representation and hence can mix and anticross) under D_{2d} are hh even with lh odd such as hh2 and lh1) or hh odd with lh even such as hh1-lh2). The lh1-hh1 coupling is forbidden. In the D_{2d}

priate C_{2v} symmetry of the single 001) interface. This approach is substantially similar to Ivchenko's. The only difference is that the lh-hh coupling parameter is expressed in terms of the valence-band offset.[27]

C. The purpose of the present paper and its main results

The purpose of this paper is to provide a microscopic atomistic theory for lh1-hh2 coupling in D_{2d}-type GaAs/ AlGa)As heterostructures. Using the empirical pseudopotential method we determine the period n_c where the $(GaAs)_n/(AlAs)_n$ superlattices and the $(GaAs)_n/(Al_{1-x}Ga_xAs)$ quantum wells exhibit lh1-hh2 anticrossing at different values x of the barrier. By varying the composition of the barrier material we alter the magnitude of the well-to-barrier valence-band offset $E_v(x)$. Calculation of the coupling matrix element vs barrier composition then establishes $V^{\mathbf{k}_\parallel=0}_{lh1,hh2}$ for different barrier heights $E_v(x)$. We find that: i) the lh1 and hh2 states anticross at rather large quantum well widths or superlattice periods $60<n_c<70$ monolayers. ii) The coupling matrix element $V^{\mathbf{k}_\parallel=0}_{lh1,hh2}$ is small, being between 0.02 meV and 0.07 meV. iii) The coupling matrix element obtained from our atomistic theory is at least an order of magnitude smaller than that inferred from the phenomenological model Hamiltonian approach of Ivchenko using a coupling parameter $t_{lh}=0.5$).[6] iv) The coupling matrix element is small at low Al composition shallow barrier)

tonian; d) one needs to fit only the bulk band structure without additional e.g., interfacial) parameters[6].

Finally, using the eigenstates obtained solving Eq. 2) we have calculated the interband dipole transitions-matrix elements squared $I_{i,j}(\hat{\ }) = |\ \ _i|\ \hat{\ } \cdot \hat{p}|\ \ _j\rangle|^2$, where $\hat{\ }$ is the photon polarization vector, $_i$ are the hh1, lh1, and hh2 hole states, while $_j$ are the $e1$ and $e2$ electron states at $\mathbf{k}_\parallel = 0$. The study of the polarization-dependent oscillator strengths of the interband transitions provide further information about the nature of the hole and electron states and state mixing.

III. RESULTS

Figure 1 shows the energies of the first three lowest hole states in $(\mathrm{GaAs})_n/(\mathrm{AlAs})_n$ superlattices versus the superlattice period n at $\mathbf{k}_\parallel = 0$. We see that the first three hole states have the order hh1, lh1, and hh2, respectively, and approach the GaAs VBM as the period n increases. On the scale of the figure it is impossible to verify any anticrossing between lh1 and hh2. Thus, Fig. 2 shows a closeup of the region in the

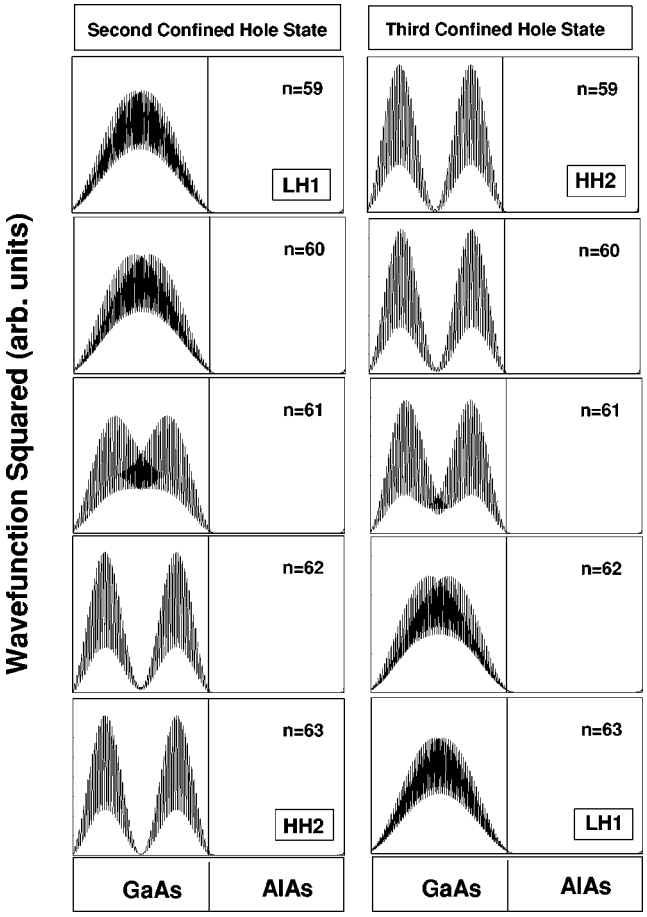

FIG. 3. Evolution of the wave functions of the second confined hole state left column) and the third confined hole states right column) of $(GaAs)_n/(AlAs)_n$ superlattices with the superlattice period n. Wave functions are averaged over the in-plane coordinates.

crossing period n_c increases from a lower value $n_c=61$ at $E_v(x=1)=489$ meV to $n_c=66$ at $E_v(x=0.1)$ 40 meV.

Figure 6 shows the anticrossing gap E_{AC} approximately twice the $V_{lh1,hh2}$ coupling parameter) versus the barrier height, $E_v(x)$. We obtain the largest value of E_{AC} at $E_v(x=0.2)=82$ meV. The corresponding coupling potential is $V_{lh1,hh2}$ 0.065 meV. Note that $V_{lh1,hh2}$ is smaller at higher E_v higher Al content in the barrier) and is 0.03 meV at $E_v=490$ meV $(x=1)$. Note also that these values for $V_{lh1,hh2}$ are larger than the value obtained in the case of $(GaAs)_n(AlAs)_n$ superlattices, 0.020 meV Fig. 2).

To understand the trend of the coupling $V_{lh1,hh2}$ versus barrier height, we refer to an expression derived by Cortez *et al.*[27] in the framework of the envelope-function description of the superlattice states:

$$V_{lh1,hh2}=\frac{E_v}{2\sqrt{3}} f_{lh1}\ z_{int})f_{hh2}\ z_{int})\frac{a}{2}. \qquad 4)$$

In this model the coupling potential is taken to be proportional to the product of the envelope-function amplitudes f_{lh1} and f_{hh2} at the interfaces z_{int} times the potential barrier value. To test this model we plot in Fig. 7 $(2V_{lh1,hh2})/(|f_{lh1}(z_{int})|\cdot|f_{hh2}(z_{int})|)$ versus $E_v(x)$. We use envelope functions f which are directly extracted from our calculated microscopic wave functions, normalized over the unit-cell volume, through a macroscopic average procedure. In this procedure the wave functions are first averaged in the xy planes orthogonal to the growth direction z to obtain $\overline{\ }(z)$. Then, to eliminate the oscillations along the z direction which are periodic with a period equal to a monolayer distance), $\overline{\ }(z)$ are averaged within every monolayer. The resulting envelopes f are then normalized over the superlattice unit cell. We evaluate the envelopes $f(z)$ corresponding to superlattices with periods $n<n_c$, i.e., far from the anticrossing period where the lh1 and hh2 envelopes could be deformed by the coupling and extrapolate at n_c. According to the model of Cortez *et al.* the slope of Fig. 7 should be constant, $a/2\sqrt{3}$. Figure 7 shows that our microscopic calculation does not produce the simple linear scaling implied by Eq. 4). The function plotted increases rapidly at low valence-band offsets whereas at large offset it saturates to a constant value.

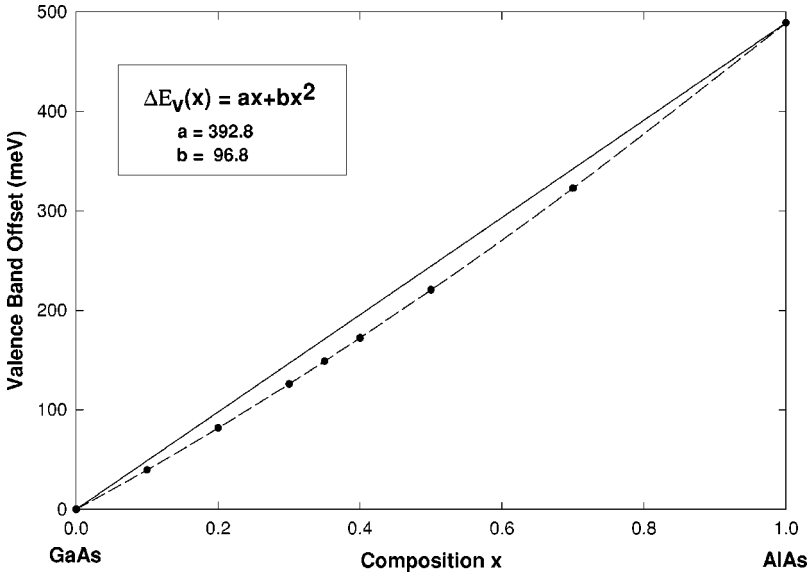

FIG. 4. Valence-band offset between the GaAs valence-band maximum and the $(Al_xGa_{1-x})As$ valence-band maximum as a function of the composition x of the barrier.

We can analyze our results for $V_{lh1,hh2}$ versus E_v as follows. For large barrier height the envelope functions are strongly localized *inside* the well, so their amplitude $f(z_{int})$ at the interfaces approaches zero, and $V_{lh1,hh2} \to 0$. For small barrier height $E_v \to 0$ there is no interface anymore, the cubic symmetry is restored, and $V_{lh1,hh2} \to 0$. Thus, there should be a value of E_v at which the coupling matrix element $V_{lh1,hh2} = |\langle lh1 | V | hh2 \rangle|$ between lh1 and hh2 is largest. From Fig. 6 we see that the value of E_v at which the coupling potential is largest is $E_v \approx 82$ meV.

agreement with the values we have obtained with our pseudopotential approach. The different n_c are related to the different bulk parameters.

Ivchenko *et al.*[6] considered a AlAs/GaAs/AlAs quantum well with a variable number n of GaAs monolayers. They introduced the lh1 and hh2 anticrossing in an *ad hoc* fashion in the envelope-function formalism through the ''generalized boundary conditions,'' which are equivalent to adding to the Hamiltonian a -function term, localized at the interfaces. The coupling potential was expressed in terms of an adimensional parameter t_{lh} multiplied by the product of the lh1 and hh2 envelope-function amplitudes at the interface. They used $m_{hh}=0.45$, $m_{lh}=0.09$, $E_v=0.53$ eV similar to our values $m_{hh}=0.40$, $m_{lh}=0.11$, $E_v=0.49$ eV). Selecting $t_{lh}=0.5$ they obtained a gap of 1–2 meV at the crossing point $n_c=50$. This gap is at least *one order of magnitude larger* than the values directly estimated in our atomistic calculations. Also, the trend of the E_{lh1} and E_{hh2} energies versus n, given in Fig. 3 a) of Ref. 6, is such that the minimum difference between them the anticrossing gap E_{AC}), is not achieved at $n=n_c$ the value of n at which lh1 and hh2 exchange their character, see also Fig. 3 c) of Ref. 6] as it is in the atomistic calculations. Obviously, the interaction potential parameter $t_{lh}=0.5$ is too strong. Our atomistic calculations show that $V_{lh1,hh2}$ is smaller, of the order of tens or hundreds of meV, and its effect on the hole energies is seen essentially only at $n \approx n_c$. At smaller or larger n, $E_{lh1}=E^0_{lh1}$ and $E_{hh2}=E^0_{hh2}$, where E^0_{lh1} and E^0_{hh2} indicate the uncoupled lh1 and hh2 energies. The differences between the model Hamiltonian approach[6] and our atomistic approach highlight the fact that the former approach depends on parameters it cannot calculate.

On the experimental side, the effect of the lh1 and hh2 coupling in D_{2d} systems is seen in the appearance of dipole-forbidden $e1$-hh2 and $e2$-lh1 exciton features.[17,18] From the excitation spectra of $(GaAs)_{36}/(Al_{0.27}Ga_{0.73}As)_{74}$ multiple quantum wells, the energy difference between the dipole-allowed e_{1l} = (lh1-$e1$) and the dipole-forbidden e_{12h} =(hh2-$e1$) excitons and between the dipole-forbidden e_{21l} =(lh1-$e2$) and the dipole-allowed e_{2h}=(hh2-$e2$) excitons can be estimated in both cases to be about 10 meV. In our single-particle calculation when the splitting between E_{lh1} and E_{hh2} is 10 meV, the light-hole and heavy-hole states are only weakly coupled. However, a calculation of a full excitonic spectrum, which is beyond our single-particle approach, would be necessary to assess the intensities of these transitions and afford a direct comparison with this experiment.

V. DIPOLE TRANSITION STRENGTHS

Figure 8 shows the dipole matrix elements for transitions from the second valence subband denoted as $V2$) and the third valence subband denoted as $V3$) to the two lowest conduction subbands, $e1$ and $e2$, for a $(GaAs)_n/(Al_{0.2}Ga_{0.8}As)_{m=74}$ quantum well, as a function of the number n of GaAs layers in the well. We see that the dipole transition probabilities show a mirrorlike behavior across the value $n_c=64.7$ which corresponds to the calculated period n_c of the anticrossing between lh1 and hh2. For $n<n_c$ the calculated transition probabilies indicate that the subband $V2$ = lh1 and $V3$ = hh2, while for $n>n_c$ the roles of $V2$ and $V3$ are exchanged. This calculation provides another way to study the mixing transition between $lh1$ and $hh2$ and determine the anticrossing point n_c. We see from this result that the transition takes place over just three monolayers. The calculations of Chang and Schulman[19] showed a much more gradual transition with the well width n.

From Fig. 8 we also see that there is a dependence of the transition probability on the polarization direction along z or in the x-y plane. The transitions to the $e2$ electron state are completely in-plane polarized while those to the $e1$ state are *mainly* polarized along z. No in-plane polarization anisotropy between the 110] and -110] directions is observed for any transitions. This can be understood by observing that the overall symmetry of these systems is the D_{2d} point group which leads to anV2are

sary values for the coupling strength. We have calculated the strength of $V_{lh1,hh2}^{\mathbf{k}_\parallel=\mathbf{0}}$ through the evaluation of the anticrossing gap which opens between the lh1 and hh2 energies when they get closer to each other. This evaluation has been performed for $(\mathrm{GaAs})_n/(\mathrm{AlAs})_n$ superlattices and for $(\mathrm{GaAs})_n/(\mathrm{Al}_x\mathrm{Ga}_{1-x}\mathrm{As})_{m=}$ quantum wells, where the Al content of the barrier x has been varied from 0.1 to 1.0. At a critical period $n=n_c$, anticrossing between the lh1 and hh2 states is calculated. Our calculations show that the strength of $V_{lh1,hh2}$ is very small, of the order of magnitude 0.05 meV, in all the systems we have studied. The smallness of this interaction causes the lh1 and hh2 states to mix and form an anticrossing gap only for periods that are within a few monolayers of the critical size n_c at which anticrossing occurs. This happens at a period $n_c^{\nwarrow}$ 61 in $(\mathrm{GaAs})_n/(\mathrm{AlAs})_n$ superlattices with a gap about 0.040 meV wide. Also in $(\mathrm{GaAs})_n/(\mathrm{Al}_x\mathrm{Ga}_{1-x}\mathrm{As})_{m=}$ multiple quantum wells the anticrossing well width n_c varies between 61 and 67 as a function of the Al barrier composition x. The anticrossing gap E_{AC} and $V_{lh1,hh2}$) depends on the composition x of the bar-